LASM/OSU

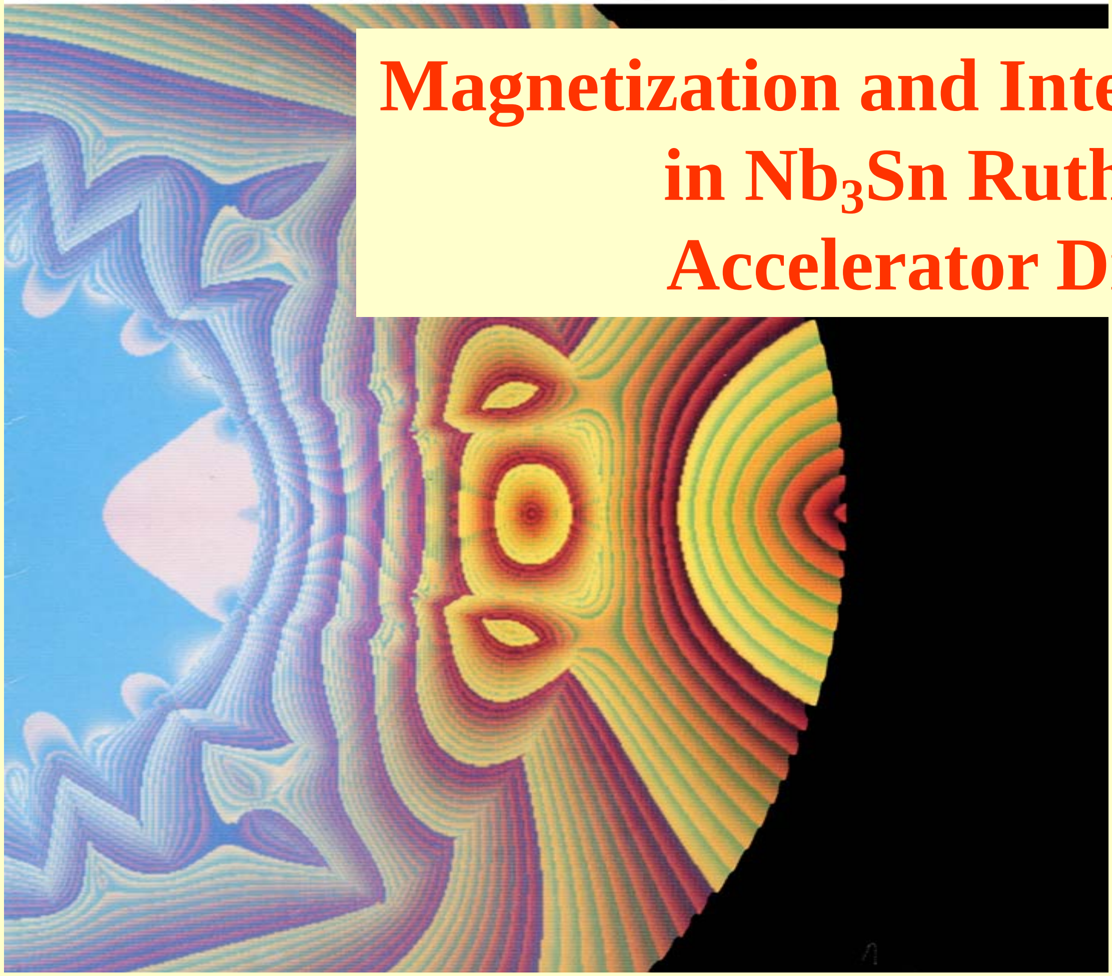

Magnetization and Interstrand Coupling in Nb_3Sn Rutherford Cables for Accelerator Dipole Applications

E.W. Collings
and
M.D. Sumption

Laboratories for Applied Superconductivity and Magnetism (LASM)
MSE/OSU

THE OHIO STATE UNIVERSITY

Department of Materials Science and Engineering

LASM THE OHIO STATE UNIVERSITY
Laboratories for Applied Superconductivity and Magnetism

A research collaboration over the years with:

LBNL, Berkeley, CA, USA
R.M. Scanlan
D.R. Dietderich
FNAL, Batavia, IL, USA
A.V. Zlobin
E. Barzi
D. Turrioni
R. Yamada
G. Ambrosio
KEK, Tsukuba, Japan
T. Shintomi
M. Wake*
S.W. Kim*
University of Twente, Enschede, ND
H.H.J. ten Kate*
A.P. Verweij*
Y. Ilyin
A. Nijhuis

** Now relocated*

Supported by the U.S. DOE Division of High Energy Physics under Grant No. DE-FG0295ER40900

Purpose of AC-Loss (Coupling) Studies

In order to ensure stability and to reduce distortions of the cable-wound dipole guidance fields of high energy particle accelerators it is important to control the magnitudes of interstrand coupling currents (ICC) and "supercurrents" (i.e. boundary-induced coupling currents, BICCs) .

Both of these are suppressed by increasing the cables' crossover and side-by-side ICRs, $R_{\perp}$ and $R_{//}$, respectively. Full strand insulation is not acceptable.

A compromise between ICC and BICC reduction and magnet stability via interstrand current sharing leads to the recommendation that **$R_{//}$ should be small and $R_{\perp}$ should be large, but not too large, i.e. about 15±5 μΩ .**

The introduction of a stainless steel core into the Nb_3Sn cable is intended to raise its as-reacted $R_{\perp}$ from the vicinity of **0.2 μΩ** into the desired range.

Fine tuning is generally achieved by varying the width of the core.

Measurement and Analysis

Magnetic and /or calorimetric measurement of the frequency dependence of loss

yields $\boldsymbol{Q_{total} \sim Q_h + Q(f)}$

The “hysteretic loss” component (persistent current magnetization)

Primarily interstrand coupling loss hence interstrand contact resistance, ICR

Q(f), the interstrand coupling component

(1) The low-frequency range

$$Q_\perp = \left(\frac{4}{3}\right)\left(\frac{w}{t}\right)L_p B_m\left[\frac{N^2}{20R_\perp}+\frac{1}{NR_\parallel}\right].\left(\frac{dB}{dt}\right) \quad = \left(\frac{2\pi^2}{3}\right)\left(\frac{w}{t}\right)L_p B_m^2\left[\frac{N^2}{20R_\perp}+\frac{1}{NR_\parallel}\right].f \qquad \textbf{(FO)}$$

$$Q_\parallel = \left(\frac{t}{w}\right)L_p B_m\left[\frac{1}{NR_\parallel}\right].\left(\frac{dB}{dt}\right) \qquad \textbf{(EO)}$$

-- hence ICR from the **initial slope, *dQ/df*,** from the **FO** measurement

$$\boxed{dQ_\perp / df = \left(\frac{\pi^2}{30}\right)\left(\frac{w}{t}\right)L_p B_m^2 N^2\left[\frac{1}{R_{\perp,eff.}}\right]}$$

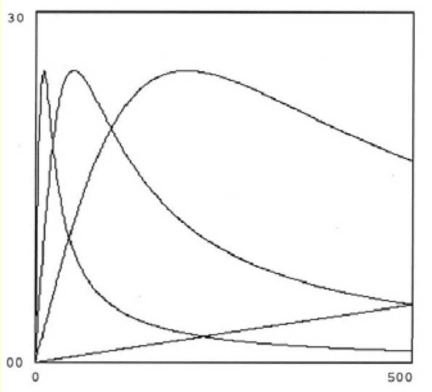

(2) The full-frequency range

$$Q(f) = Q_0\frac{f/f_c}{1+(f/f_c)^2}$$

-- hence ICR from the **"critical frequency", *f_c***

$$\boxed{R_{\perp,fc} = 2\pi(DE)\,f_c}$$

$Q_{coupling}(f)$ characteristics, each figure representing three cables

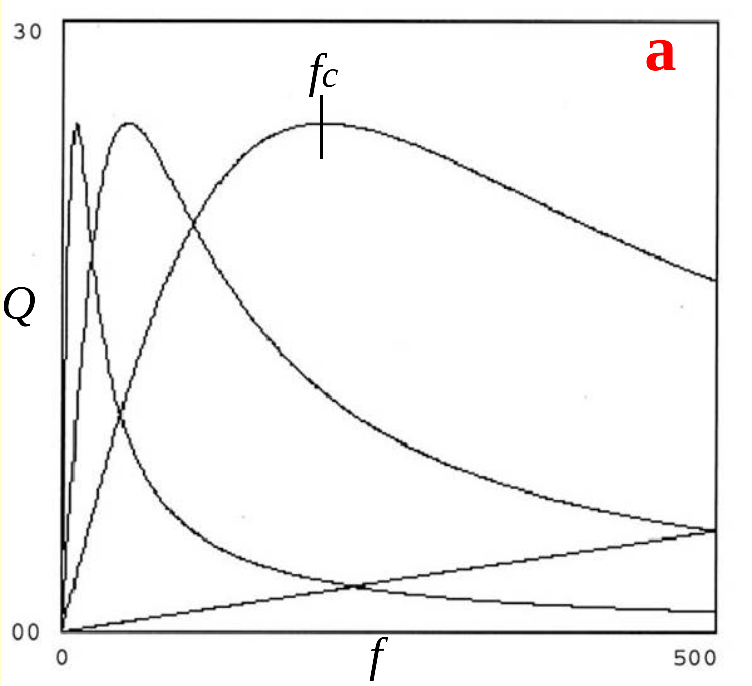

(a) Each cable has a single homogeneous ICR, each given by its initial slope ***dQ/df*** and/or its critical frequency, f_c

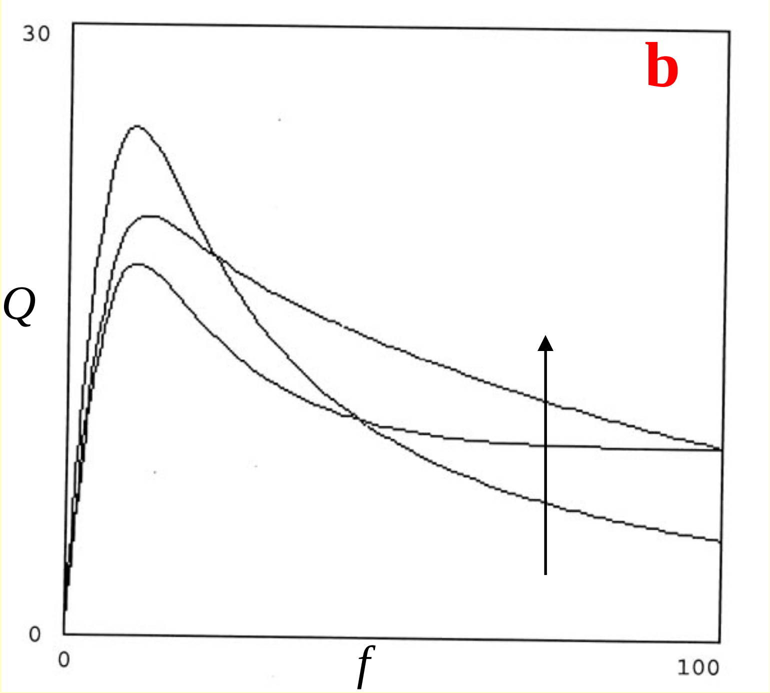

(b) Each cable exhibits a blend of two ICRs, one common to all cables and the other different for each cable. Thus each curve possesses a second f_c that elevates its tail

Pioneering investigations on cored NbTi cables provided the basis for subsequent studies of cored Nb_3Sn research-type-, LARP-, and NED cables

NbTi Cables: Background studies

strand coating in general
stabrite coating
introduction of the core
influence of compaction
variation of core width

Nb_3Sn Cables: Coupling Loss and ICR

strand architecture
external- and internal (core) copper
stainless steel cores – monolithic and bimetallic
variation of pre-heat treatment condition
variation of cable (magnet) preparation conditions

Nb_3Sn Cables: Magnetization, ICR, and *deff*

variation of core width and placement
importance of strand magnetization

Background -- NbTi Cables

Problem: Coupling loss in SSC’s fast-ramping HEB dipoles

Study group-1
Subsize cables with variously coated strands
strand coatings of Cr, Ni, Ni+Cr, Ni-P

Study group-2
Cables with various strand coatings and cores
bare-Cu, Ni-plated, stabrite coated strands
cores of titanium, stainless steel, kapton
three "curing" temperatures
measured with and without cold pressure, 36 and 78 MPa

Background -- NbTi Cables

Problem: Magnetization and Coupling in LHC dipoles

Study group-3
Bare-Cu cables with and without SS cores

- stainless steel cores, three thicknesses ("internal compaction")
- three curing temperatures
- measured under "pressure-release"

Study group-4
Stabrite coated cables with and without SS cores

- two core thicknesses
- five core widths (including zero width)
- four levels of external compaction
- several "curing" temperatures

Suppression of Coupling Loss in Cored NbTi Cables

(1) Introduction of a full core completely suppresses crossover contact in bare-Cu and stabrite-cored cables

(2) Extreme sensitivity of stabrite cables to cold pressure is eliminated by the introduction of the core

(3) The effective field-perp. contact resistance can be adjusted by varying the width of the SS core

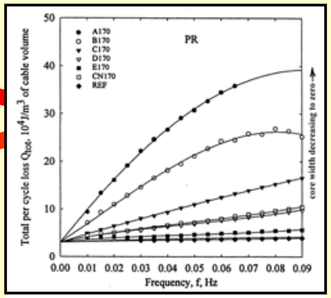

Loss suppression in a bare-Cu cable using a full-width core.

Note the effect of “internal compaction” (variation of core thickness)
and change of curing temperature (200-250^{o}C)

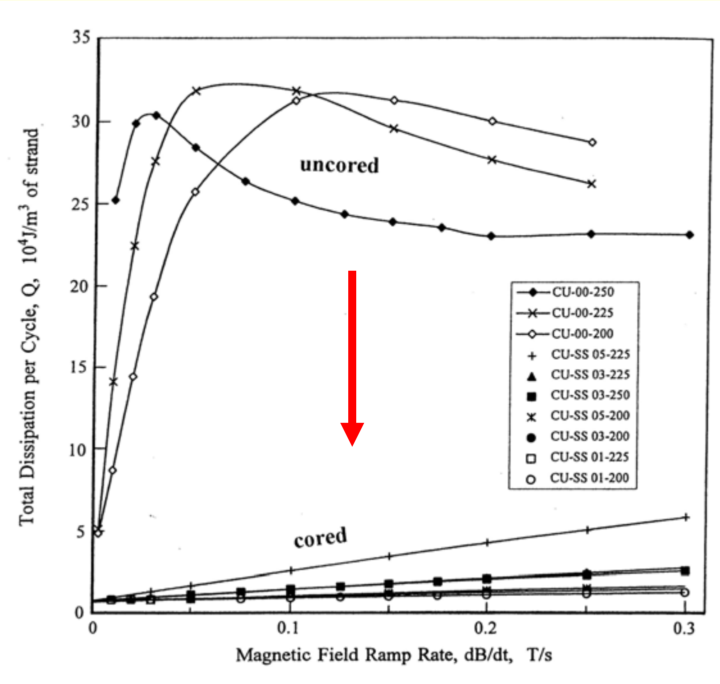

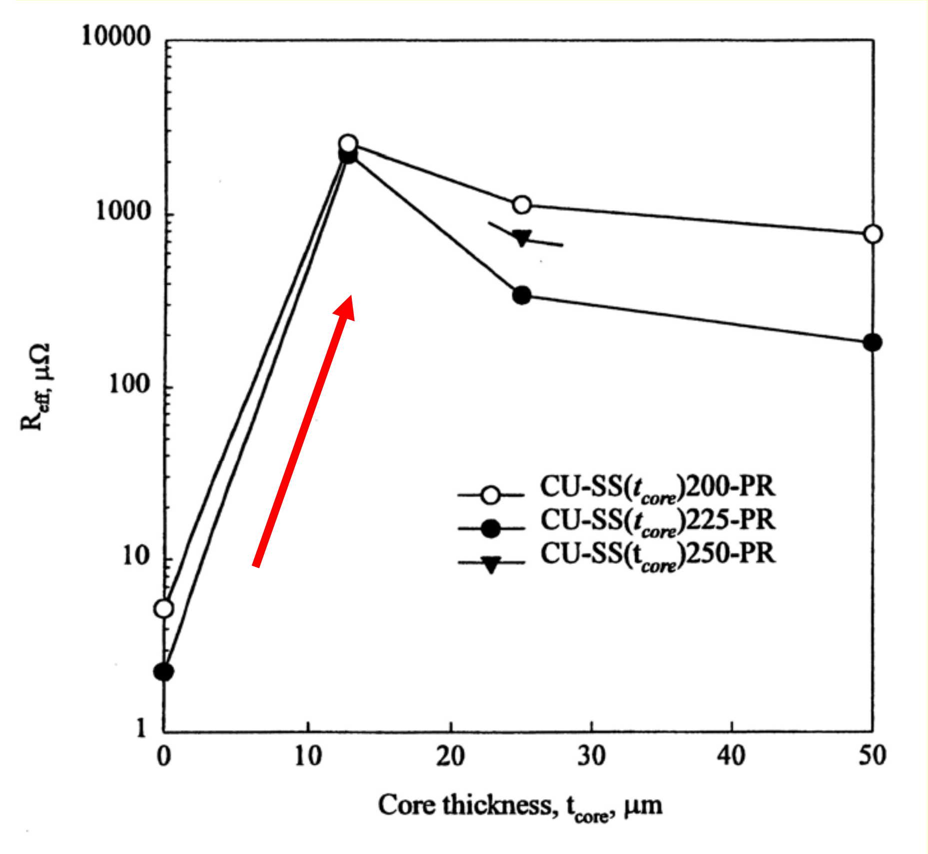

Stabrite coated cables respond strongly to increases in cold pressure

ST170/0, 35, and 78MPa

SS-cored stabrite cables are insensitive to cold pressures in the range 0 - 78 MPa

ST170SS/0,35, and 78 MPa

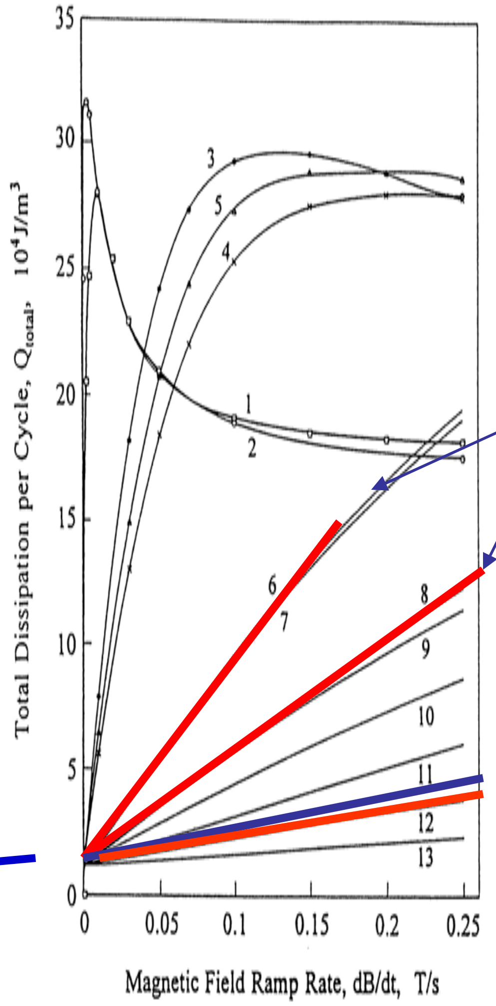

Figure 1.
Total energy dissipation per cycle versus field ramp rate‡.

1. CU250A
2. CU250B
3. ST200
4. ST200/3days†
5. ST200/3days/78MPa
6. ST150/78MPa
7. ST170/78MPa
8. ST170/36MPa
9. ST150/36MPa
10. ST-SS200
11. NI250
12. ST-SS150
13. CU170

Control of ICR by variation of core width

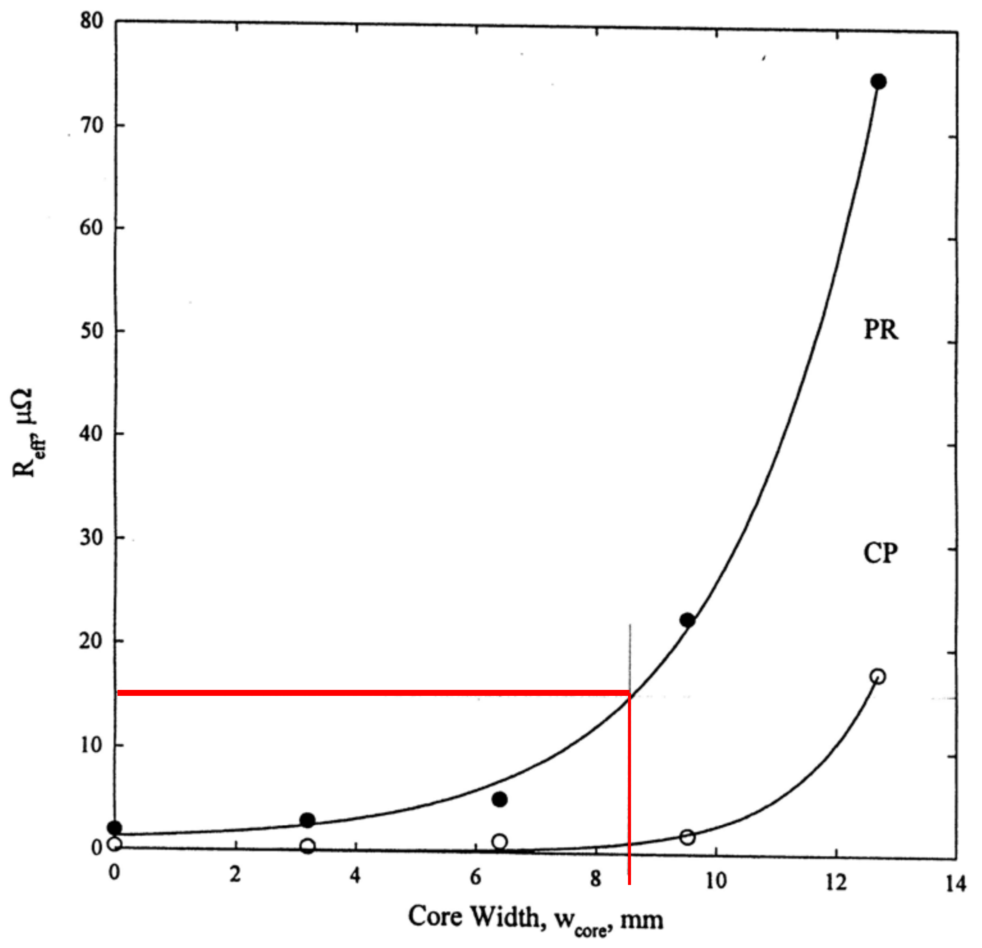

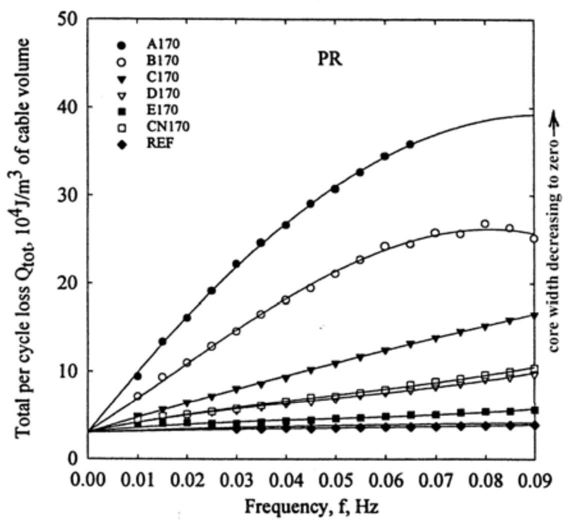

No core

Full core

Target $R_{eff} = 15\ \mu\Omega$

AC Loss in Nb$_3$Sn Cables

(1) Coupling Loss and Interstrand Contact Resistance

Variation of strand architecture

Introduction of external- and internal (core) copper

Introduction of stainless steel cores – monolithic and bimetallic

Variation of pre-heat-treatment condition

Variation of cable (magnet) preparation conditions

Variation of core width and placement

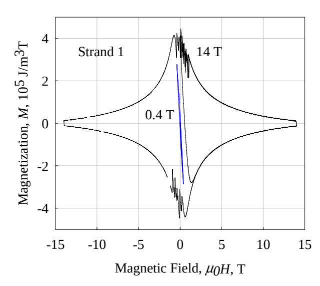

(2) Cable and Strand Magnetization, ICR, and d_{eff}

Coupling Loss and ICR
-- core suppression of loss

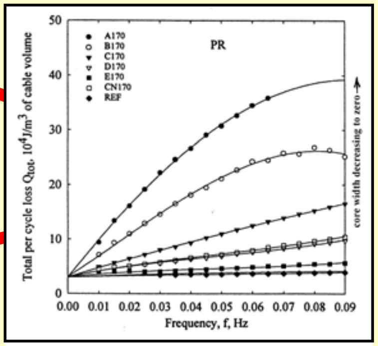

Typical Results *– measurements made at University of Twente by MDS*

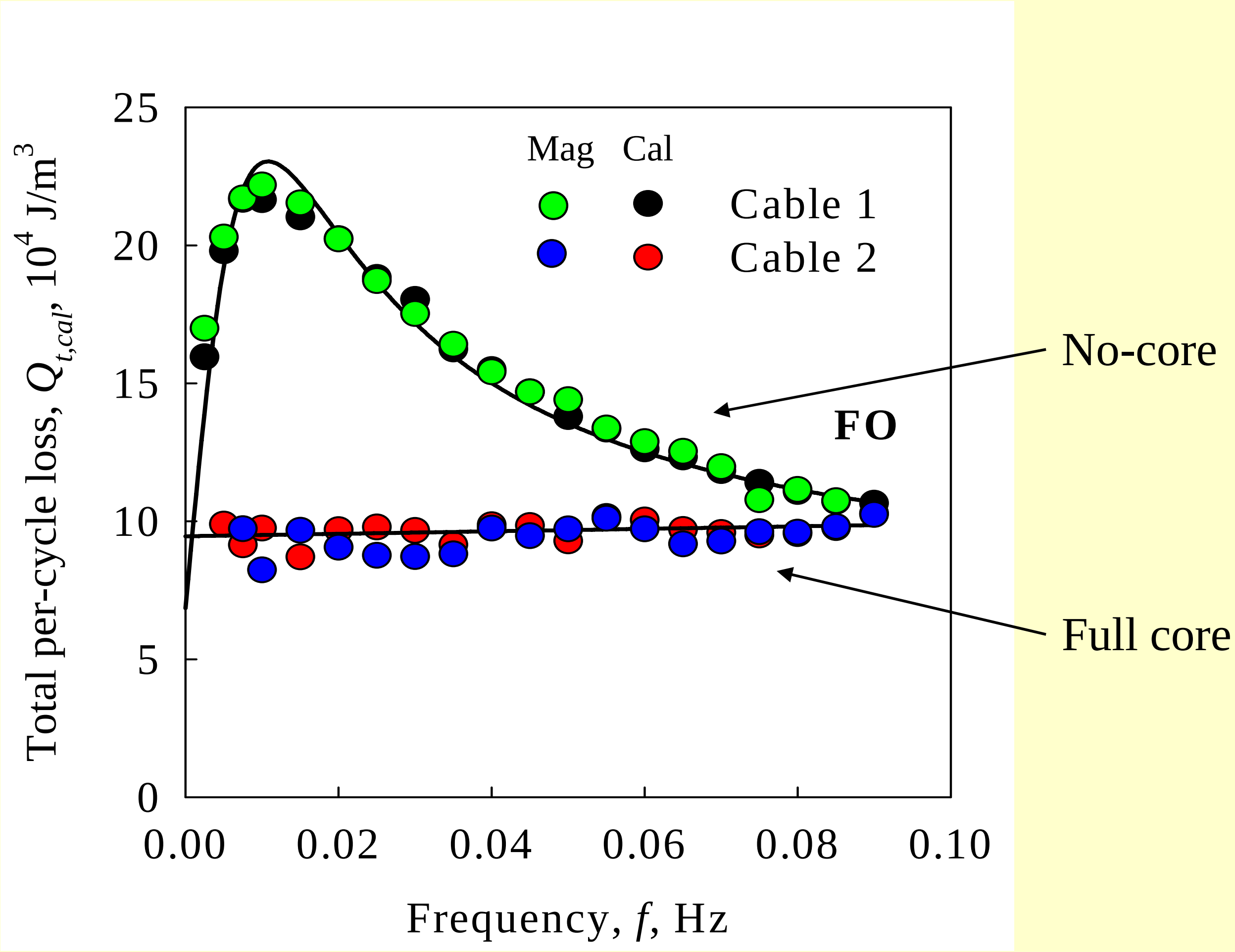

Collected Results, $R_{\perp,eff}$, μΩ

	No core	Full-Width Core
[2]	<0.1 (0T), 2.7 (1T)	33 (0T), 78 (1T)
[5]	0.24	23
		24
		53
		“∞”
[6][7]	0.15 (0T), 0.4 (1T)	
	13.0 (0T), 11.5 (1T)	
	1.47 (0T), 3.09 (1T)	
	0.33 (0T), 1.27 (1T)	
	0.30 (0T)	
[8]	0.4 and 4	
[9]	0.19, 0.21	8
[11]	0.31	209

“Averages” 0.7 (0T), 1.9 μΩ (1T) 33 → more than 200 μΩ

Coupling Loss and ICR
-- variation of core width

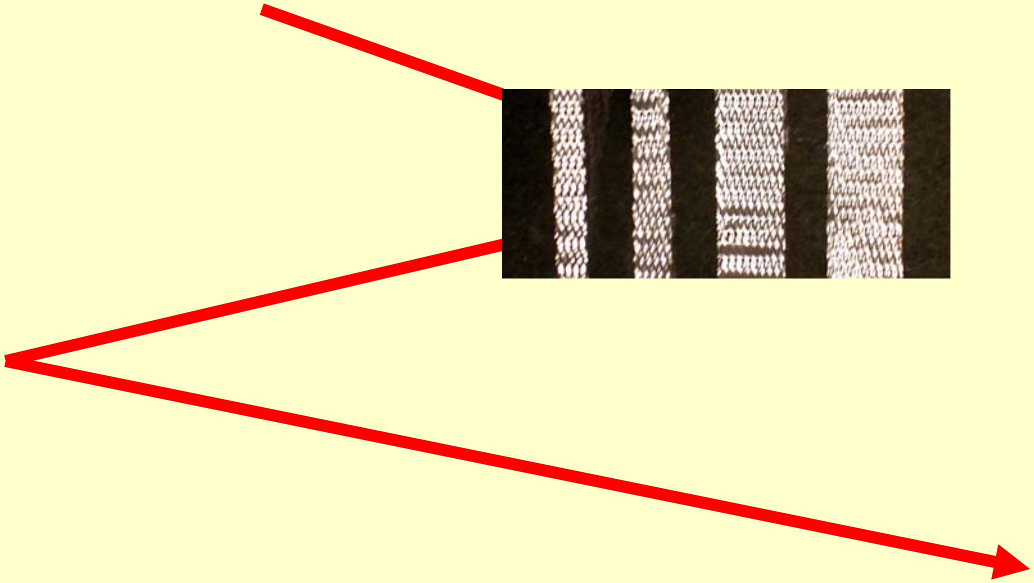

Cores removed from as-wound unreacted cables

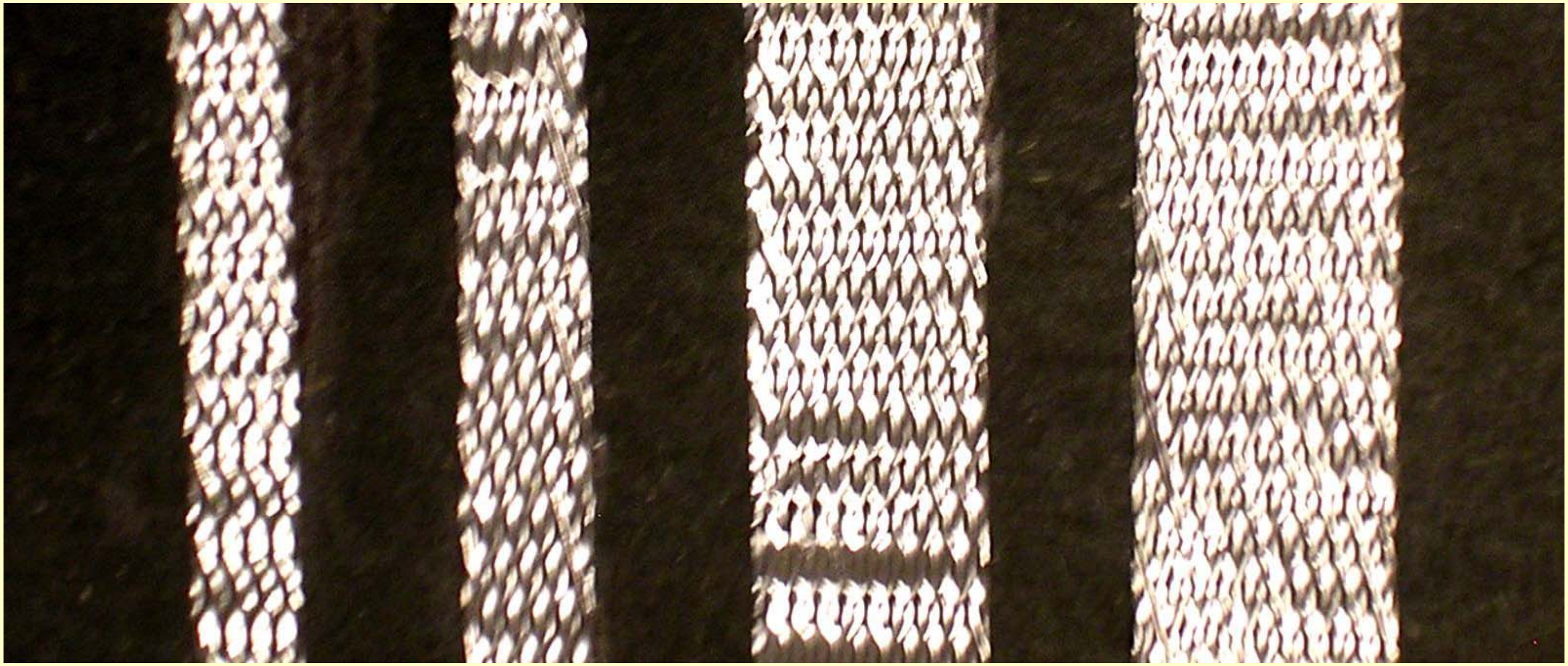

Core 4
4.5 mm

Core 5
5.2 mm

(9.5 mm)

Core 6
10.8 mm

Variation of core width [9][10]

OSU Cable No.	Core Width mm	$\langle R_{\perp} \rangle_{AV.}$ Calorimetric μΩ	$\langle R_{\perp} \rangle_{AV.}$ Magnetic μΩ	**Core placement**
3	NC	**0.19**	**0.21**	
4	4.5	**0.45**	**0.37**	**Well centered**
5	5.2	**0.29**	**0.33**	**Way off-center**
6	10.8	**8.2***	**7.90***	**Off-center**

* Based on cored-stabrite-cable results a coverage increase of from 75% to 100% could results in an almost 4-fold increase in $R_{\perp,eff.}$ – to about **32 μΩ** in this case. An even greater increase would accompany correct centering of the core.

In fact LBNL's full well-centered core yielded an $R_{\perp,eff.}$ of **209 μΩ**

Cable and Strand Magnetization, ICR, and d_{eff}

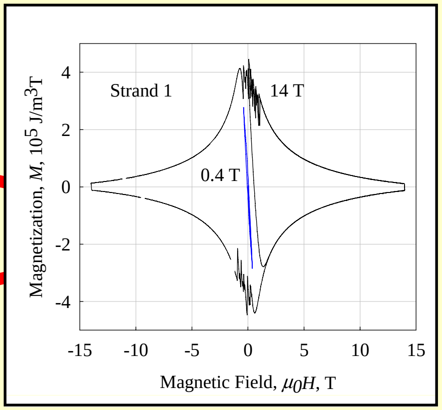

EO: 4.23 (cable, extrap.) ⟶ 4.29 (strand, VSM), $Q_h(1)$

EO: 3.62 (cable, extrap.) ⟶ 4.19 (strand, VSM), $Q_h(2)$

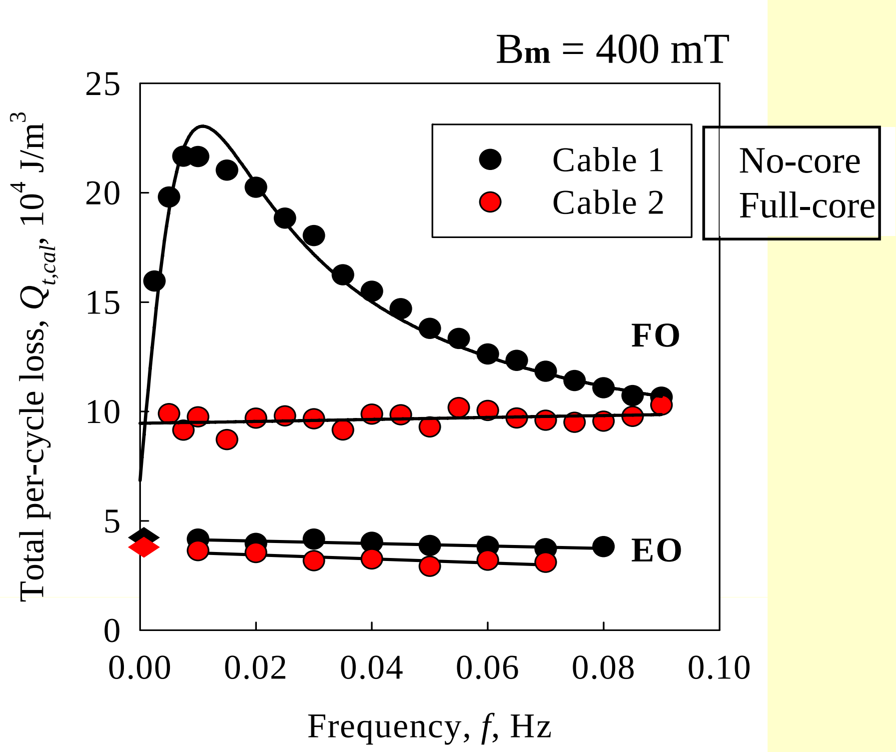

The edge-on (EO) cable loss is hysteretic (independent of ***f)*** and stems from the hysteretic losses of the individual strands in the cable pack

-- note the EO/FO anisotropy in the hysteretic loss

EO: 4.23 (cable, extrap.) → 4.29 (strand, VSM), $Q_h(1)$

EO: 3.62 (cable, extrap.) → 4.19 (strand, VSM), $Q_h(2)$

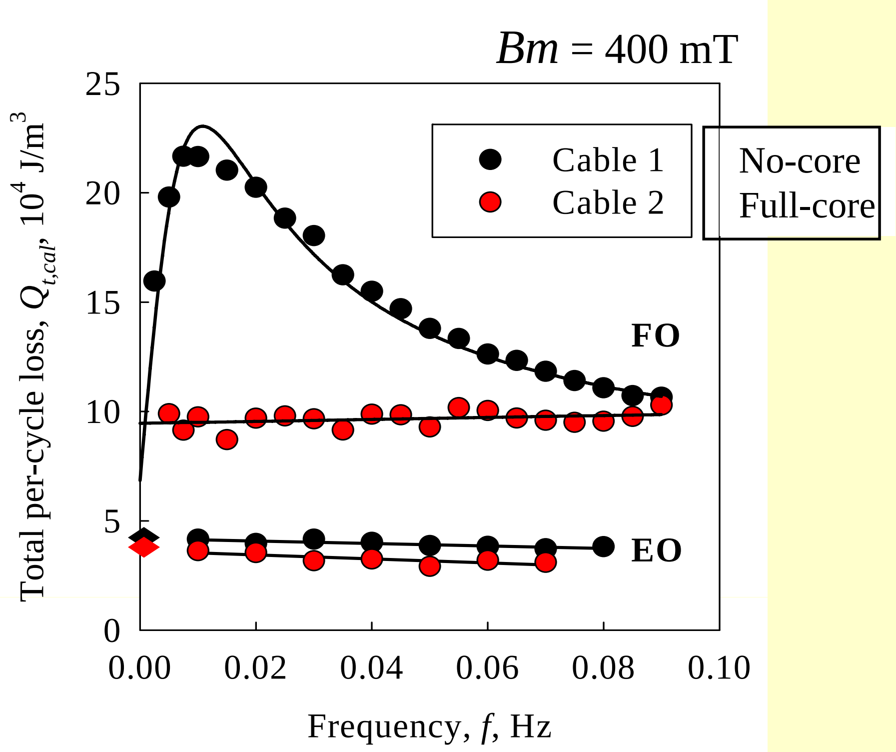

Frequency equivalent of the injection ramp-rate

$$f = 2\frac{(dB/dt)}{\pi^2 B_m}$$

Then with:

dB/dt = 7 mT/s

Bm = 400 mT

$$\boxed{f = 3.5 \text{ mHz}}$$

The edge-on (**EO**) cable loss is hysteretic (independent of ***f)*** and stems from the hysteretic losses of the individual strands in the cable pack

-- even **FO**, the coupling loss during the injection ramp (to 540 mT for LHC) would be dominated by ***Q_h***

Cable Magnetization due to Interstrand Coupling

$$Q_\perp = \left(\frac{4}{3}\right)\left(\frac{w}{t}\right)L_p B_m \left(\frac{dB}{dt}\right)\left[\frac{N^2}{20R_{\perp,eff}}\right] = 4M_{coup}B_m$$

$$M_{coup} = \left(\frac{1}{3}\right)\left(\frac{w}{t}\right)L_p \left(\frac{dB}{dt}\right)\left[\frac{N^2}{20R_{\perp,eff}}\right]$$

Next, insert a set of typical cable parameters:

w (mm)	14.23
t (mm)	1.78
(w/t)	7.99
L_p (mm)	= 55.1 mm = 0.0551 m
dB/dt (mT/s) = 7	= 0.007 T/s

$$\boxed{M_{coup} = \frac{3.774x10^4}{R_{\perp,eff}(\mu\Omega)} \qquad \text{(A/m)}}$$

Cable Magnetization based on Persistent-Current Magnetization of component strands

$$M_{cab} = \left(\frac{2}{3\pi}\right) J_{c,cab,0.5T}\,(A/m^2) \times d\,(m)$$ (Bean, in A/m)

with $J_{c,cab,0.5T} = 0.5 \text{ x } 0.9 \text{ x } 16.8 \text{ x } J_{c,non\text{-}Cu,12T}$

$$M_{cab} = 1.60 \text{ x } J_{c,non\text{-}Cu,12T}\,(A/mm^2) \times d_{eff}(\mu m)$$ (A/m)

Finally, after equating M_{coup} to M_{cab} we find:

$$\boxed{R_{\perp,eff}\,(\mu\Omega) = \frac{2.359x10^4}{J_{c,non-Cu,12T}\,(A/mm^2)\,d_{eff}\,(\mu m)}}$$

"Effective ICR" as function of filament diameter -- based on measured and deduced cable magnetizations

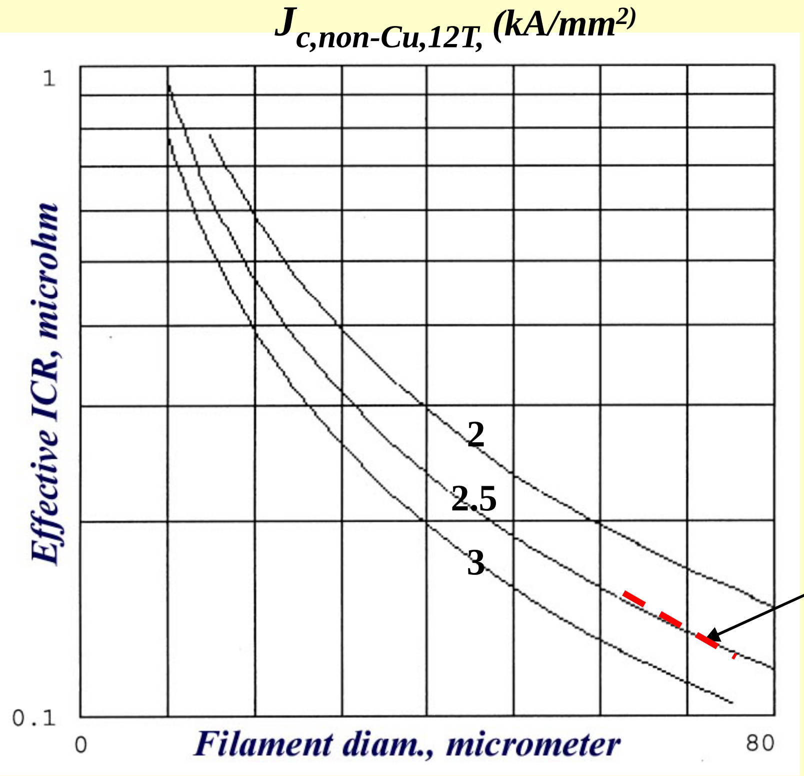

d_{eff}, μm	ICR, μΩ
30	0.32
50	0.19
100	0.09

Cable Magnetization based on Persistent-Current Magnetization of component strands at high fields, e.g., > 12 T

As the field increases from 0.5 T to > 12 T J_c decreases by a factor of > 16.8 (based on the previously used Kramer factor). At the same time the transport current needed to achieve these fields reduces the strand magnetization by a factor of $(1-i^2)$.

Let us assume $i = 0.8$. Applying the product of these reduction factors (x 46.7) to the results of the previous $M_{cab} = M_{coup}$ equality would raise $R_{\perp,eff}$ from say 0.3 μΩ (d_{eff} = 40 μm) to 14 μΩ which is within the range of accessible values.

Summary

(1) NbTi-cable studies pointed the way by showing how:
  (i) The introduction of a full-width SS core could strongly suppresses coupling loss and the crossover ICR known also as *Rc*.
  (ii) The core-suppressed *Rc* could be tuned by vary the width of the core.

(2) The above ideas were transferred into the Nb_3Sn cable program wherein it was again shown that strong loss suppression and increased ICR would accompany the introduction of SS cores and composite cores of SS and Cu.

(3) In experiments on a set of Nb_3Sn cables with cores of various widths it was found that:
  (i) ICR varied rapidly with core width
  (ii) Narrow cores produced little loss suppression
  (iii) The level of suppression was sensitive to the position of the core indicating that care is needed to ensure that the core is well centered.

(4) The EO loss tended to be frequency independent and hence attributable to the "hysteretic" persistent-current magnetization of the strands

(5) Under LHC injection conditions, B_{inj} = 540 mT and $(dB.dt)_{inj}$ = 7 mT/s, strand magnetization also dominates the FO magnetization of the Nb_3Sn cable. This was not the case for NbTi

(6) Away from injection, and in the operating field range of the dipole, the cable's magnetization drops by a factor of at least 47 into an acceptable range of values.

Acknowledgements:

LBNL, Berkeley, CA, USA

- R.M. Scanlan
- D.R. Dietderich

FNAL, Batavia, IL, USA

- A.V. Zlobin
- E. Barzi
- D. Turrioni
- R. Yamada
- G. Ambrosio

KEK, Tsukuba, Japan

- T. Shintomi
- M. Wake*
- S.W. Kim*

University of Twente, Enschede, ND

- H.H.J. ten Kate*
- A.P. Verweij*
- Y. Ilyin
- A. Nijhuis

***** Now relocated***

Supported by the U.S. DOE Division of High Energy Physics under Grant No. DE-FG0295ER40900

References

[1] AC loss and contact resistance in Nb3Sn Rutherford cables with and without a stainless steel core
M.D. Sumption, E.W. Collings, R.M. Scanlan, et al., *Adv. Cryo. Eng. (Materials)* **44** 1077-1084 (1998)

[2] Core-suppressed AC loss and strand-moderated contact resistance in a Nb3Sn Rutherford cable
M.D. Sumption, E.W. Collings, R.M. Scanlan, et al., *Cryogenics* **39** 1-12 (1999)

[3] External stabilization of Nb3Sn Rutherford cables – AC loss and contact resistance
E.W. Collings, M.D. Sumption, R.M. Scanlan, et al., *Adv. Cryo. Eng. (Materials)* **48** 1153-1160 (2002)

[4] AC loss of Nb3Sn-based Rutherford cables with internally and externally added Cu
M.D. Sumption, E.W. Collings, R.M. Scanlan, et al., *IEEE Trans. Appl. Supercond.* **13** 2376-2379 (2003)

[5] Magnetic, calorimetric, and transport studies of coupling and interstrand contact resistance in Nb3Sn Rutherford cables with bimetallic cores of stainless steel bonded to copper
M.D. Sumption, R.M. Scanlan, Yu.A. Illyin, et al., *Adv. Cryo. Eng. (Materials)* **50** 781-788 (2004)

[6] Influence of pre-heat-treatment condition on interstrand contact resistance in Nb3Sn Rutherford cables by calorimetric AC-loss measurement
E.W. Collings, M.D. Sumption, D.R. Dietderich, et al., *Adv. Cryo. Eng.(Materials)* **52** 851-858 (2006)

[7] Magnetic measurements of interstrand contact resistance in Nb3Sn cables in response to variation of pre-heat-treatment condition
E.W. Collings, M.D. Sumption, D.R. Dietderich, et al., *IEEE Trans. Appl. Supercond.* **16** 1200-1203 (2006)

[8] Interstrand contact resistance in Nb3Sn cables under LARP-type preparation conditions
E.W. Collings, M.D. Sumption, G. Ambrosio, et al., *IEEE Trans. Appl. Supercond.* **17** 2494-2497 (2007)

[9] Magnetic measurements of AC loss in cored Nb3Sn Rutherford cables – interstrand contact resistance as function of core width
E.W. Collings, M.D. Sumption, E. Barzi, et al., *Adv. Cryo. Eng. (Materials)* **54** 285-292 (2008)

[10] Effect of core width, placement, and condition on calorimetrically measured AC loss and interstrand contact resistance of stainless-steel-cored Nb3Sn Rutherford cables
E.W. Collings, M.D. Sumption, E. Barzi, et al., Proc. **MT20**, *IEE Trans. Appl. Supercond.* – to be published

[11] Influence of a stainless steel core on coupling loss, interstrand contact resistance, and magnetization of an Nb3Sn Rutherford cable
E.W. Collings, M.D. Sumption, M.A. Susner, et al., Proc. **MT20**, *IEE Trans. Appl. Supercond.* – to be published